Liquid Crystals
Publication details, including instructions for authors and subscription information:
http://www.informaworld.com/smpp/title~content=t713926090

Synthesis and mesomorphic properties of new chiral banana-shaped liquid crystals with chiral 3-(alkoxy)propoxy terminal groups

Seng Kue Lee[a]; Chang Won Park[a]; Jong Gun Lee[a]; Kyung-Tae Kang[a]; Koushi Nishida[b]; Yoshio Shimbo[b]; Yoichi Takanishi[b]; Hideo Takezoe[b]
[a] Department of Chemistry and Chemistry Institute for Functional Materials, Pusan National University, Pusan 609-735, Korea [b] Department of Organic and Polymeric Materials, Tokyo Institute of Technology, Meguro-ku, Tokyo 152-8552, Japan

To cite this Article Lee, Seng Kue , Park, Chang Won , Lee, Jong Gun , Kang, Kyung-Tae , Nishida, Koushi , Shimbo, Yoshio , Takanishi, Yoichi and Takezoe, Hideo(2005) 'Synthesis and mesomorphic properties of new chiral banana-shaped liquid crystals with chiral 3-(alkoxy)propoxy terminal groups', Liquid Crystals, 32: 10, 1205 — 1212
To link to this Article: DOI: 10.1080/02678290500303056
URL: http://dx.doi.org/10.1080/02678290500303056

Liquid Crystals, Vol. 32, No. 10, October 2005, 1205–1212

Synthesis and mesomorphic properties of new chiral banana-shaped liquid crystals with chiral 3-(alkoxy)propoxy terminal groups

SENG KUE LEE†, CHANG WON PARK†, JONG GUN LEE†, KYUNG-TAE KANG*†, KOUSHI NISHIDA‡, YOSHIO SHIMBO‡, YOICHI TAKANISHI‡ and HIDEO TAKEZOE‡

†Department of Chemistry and Chemistry Institute for Functional Materials, Pusan National University, Pusan 609-735, Korea

‡Department of Organic and Polymeric Materials, Tokyo Institute of Technology, O-okayama 2-12-1, Meguro-ku, Tokyo 152-8552, Japan

New chiral banana-shaped liquid crystals with chiral 3-(alkoxy)propoxy terminal groups (P*n*-O-PIMB5*-4O, *n*=7, 8, 9 and 10) were synthesized and their mesomorphic properties and phase structures investigated by means of electro-optic measurements, polarizing optical microscopy, differential scanning calorimetry, and second harmonic generation measurements. Most of these chiral bent-core mesogens (*n*=7–9) showed the antiferroelectric B2 phase, whereas P10-O-PIMB5*-4O exhibited the B7 phase. Comparing with the previously reported homologue P*n*-O-PIMB(*n*-2)*, we conclude that the terminal chain structure, particularly the position of chiral centres, plays an important role in the emergence of particular phase structures.

1. Introduction

Ferroelectricity [1] and antiferroelectricity [2] in liquid crystals are usually observed for molecules carrying a chiral carbon. This molecular chirality was assumed to be necessary to break down the symmetry of mirror planes and create ferroelectric or antiferroelectric ordering. However, Niori *et al*. discovered that bent-core (banana-shaped) mesogens without molecular chirality can also form polar smectic layers and exhibit ferroelectric and antiferroelectric behaviour [3]. Since this discovery, the mesomorphic properties of bent-core achiral molecules have been studied extensively [4–8]. Bent-core mesogens with chiral terminal groups have also been prepared in order to investigate the role of terminal chains in phase structure [9–12]. Most achiral and chiral bent-core mesogens exhibit the antiferroelectric mesophase; only a few ferroelectric bent-core mesogens have been reported [13–21]. Watanabe *et al*. synthesized chiral banana-shaped molecules 1,3-phenylene bis[4-(4-alkoxyphenyliminomethyl)]benzoates [P*n*-O-PIMB(*n*-2)*] with chiral terminal alkyl chains $CH_3CH_2C^*H(CH_3)(CH_2)_mO$-(*n*=*m*+3). In the homologue the position of the chiral carbon with respect to the mesogenic core and the number of carbons in the terminal chains were varied. They found that the terminal chains play a crucial role in the emergence of particular phase structures: P7-O-PIMB5* exhibits a stable antiferroelectric phase while the stable state of P8-O-PIMB6* is ferroelectric [5, 10, 21–23].

Recently we found an odd–even effect for the emergence of the ferroelectric and antiferroelectric states in two homologous series: P*n*-O-PIMB(*n*-2)* (*n*=6–10) and their oxygen analogues P*n*-O-PIMB(*n*-2)*-(*n*-4)O (*n*=8, 9, and 10) with ω-[(*S*)-2-methylbutoxy terminal groups [24]. In this report, we describe the synthesis of new chiral banana-shaped liquid crystals (P*n*-O-PIMB5*-4O, *n*=7, 8, 9 and 10) with chiral 3-(alkoxy)propoxy terminal groups $CH_3(CH_2)_mC^*H(CH_3)O(CH_2)_3O$– (*n*=*m*+6) where the position of the chiral carbon with respect to the mesogenic core is fixed and only the length of terminal chain is varied. We investigated their mesomorphic properties and phase structures by means of electro-optic, polarization reversal current, and second harmonic generation (SHG) measurements in order to study the effect of terminal chains on the phase structure.

2. Experimental

2.1. *Measurements*

^{1}H NMR spectra were recorded on Varian Gemini-200 (200 MHz) and Varian Inova (500 MHz) spectrometers using chloroform as an internal standard. The latter instrument was also used for recording ^{13}C NMR spectra in $CDCl_3$ (solvent and internal reference). The

*Corresponding author. Email: kytkang@pusan.ac.kr

Liquid Crystals
ISSN 0267-8292 print/ISSN 1366-5855 online © 2005 Taylor & Francis
http://www.tandf.co.uk/journals
DOI: 10.1080/02678290500303056

samples were sandwiched between glass substrates with ITO electrodes. The thickness was in the range 2.1–5.5 μm. The cells were kept on a hot stage (Mettler FP90) for constant temperature. The texture observation was made under crossed polarizers using polarizing optical microscopy (POM) (Nikon OPTIPHOTPOL) and transition temperatures were determined by differential scanning calorimetry (DSC) using a Perkin-Elmer DSC 7 calorimeter. The polarization reversal current was measured by applying a triangular wave voltage. SHG intensity was observed by the oblique incidence (45°) of a p-polarized fundamental wave from a Nd:YAG laser (Quanta-Ray, DCR-11) to the cells. Signals were detected with a photomultiplier tube (Hamamatsu R-955) after passing through appropriate optical filters, and output signals were accumulated by a BOXCAR system (Stanford Research Systems). The measurements were carried out during the application of a triangular wave field of 10 Hz with an amplitude of 15 $V\,\mu m^{-1}$.

2.2. *Synthesis*

The synthetic route to the target compounds is illustrated in scheme 1.

2.2.1. Allyl (*S*)-2-butyl ethers, 2. Sodium hydride (60% dispersion in mineral oil, 2.95 g, 73.7 mmol) was washed by decantation with dry THF (20 ml) and suspended in DMF (40 ml). To the suspension, (*S*)-2-butanol (**1a**, 3.64 g, 49.1 mmol) was added dropwise at 0°C. After stirring for 1 h, allyl bromide (5.95 g, 49.1 mmol) in DMF (25 ml) was added dropwise and the mixture heated to reflux for 12 h. The reaction mixture was

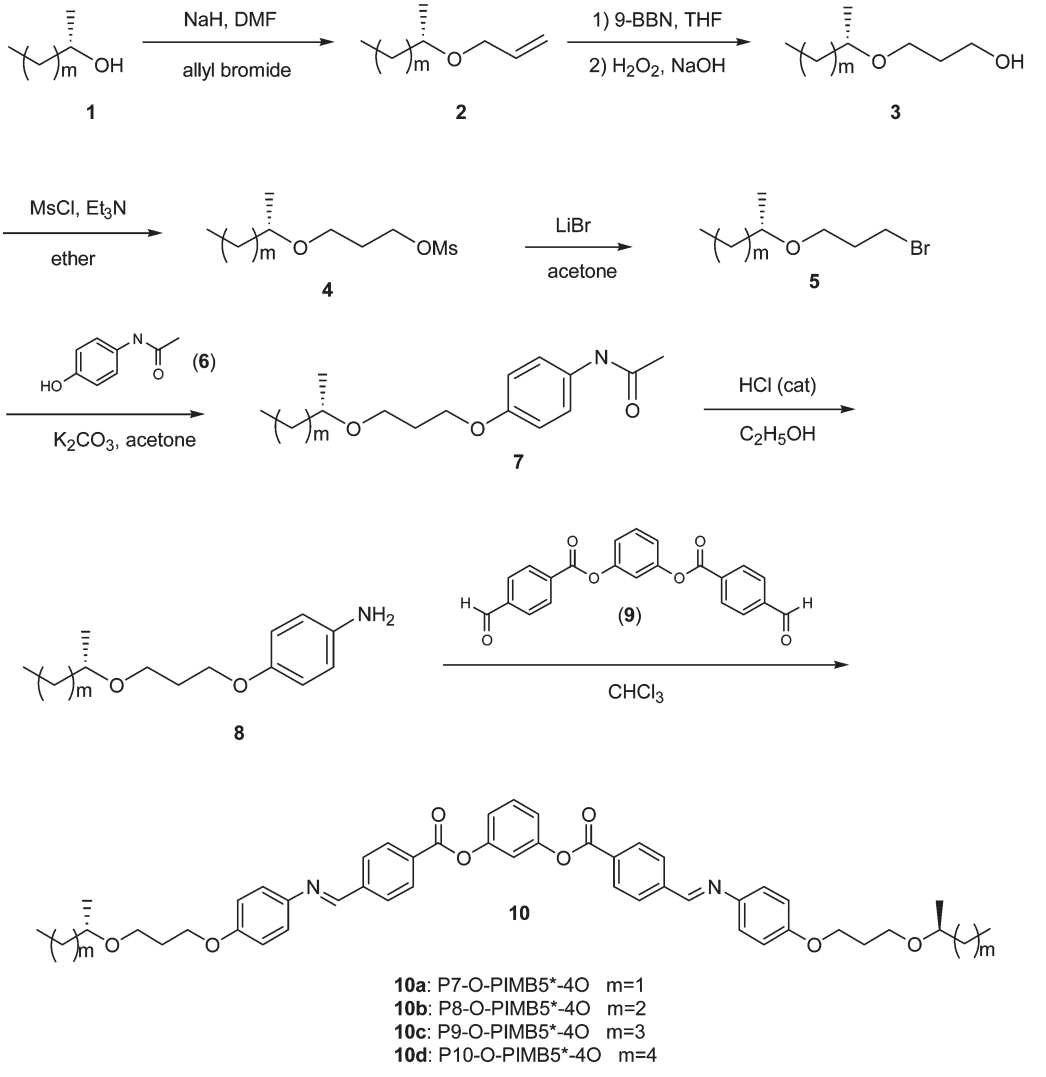

Scheme 1.

quenched by adding aqueous 1N HCl (25 ml) and extracted with diethyl ether (40 ml × 3). The combined extracts were washed with water, dried over Na_2SO_4 and concentrated to give 4.77 g (85%) of allyl ether **2a**. Compounds **2b**, **2c** and **2d** were similarly prepared in 77%, 79% and 77% yield, respectively. **2a**: ^{1}H NMR δ 0.91 (t, 3H, J=7.4 Hz), 1.14 (d, 3H, J=6.2 Hz), 1.37–1.58 (m, 2H), 3.34–3.43 (m, 1H), 3.94–4.03 (m, 2H), 5.12–5.32 (m, 2H), 5.87–6.00 (m, 1H). **2b**: ^{1}H NMR δ 0.92 (t, 3H, J=6.6 Hz), 1.15 (d, 3H, J=6.2 Hz), 1.22–1.59 (m, 4H), 3.41–3.51 (m, 1H), 3.88–4.10 (m, 2H), 5.12–5.34 (m, 2H), 5.84–6.01 (m, 1H). **2c**: ^{1}H NMR δ 0.90 (t, 3H, J=6.6 Hz), 1.14 (d, 3H, J=6.2 Hz), 1.17–1.62 (m, 6H), 3.38–3.56 (m, 1H), 3.86–4.09 (m, 2H), 5.01–5.31 (m, 2H), 5.83–6.02 (m, 1H). **2d**: ^{1}H NMR δ 0.89 (t, 3H, J=6.4 Hz), 1.14 (d, 3H, J=6.2 Hz), 1.18–1.57 (m, 8H), 3.39–3.54 (m, 1H), 3.88–4.09 (m, 2H), 5.12–5.33 (m, 2H), 5.84–6.03 (m, 1H).

2.2.2. (*S*)-3-(2-Alkoxy)propan-1-ols, 3. To a THF (7 ml) solution of allyl ether **2a** (4.70 g, 41.1 mmol), was added 9-BBN (0.5 M solution in THF, 82 ml, 41.1 mmol). The mixture was heated under reflux overnight and cooled to room temperature. To this solution were added ethanol (30 ml), and 4N aqueous NaOH (30 ml) and 30% aqueous H_2O_2 (30 ml) added dropwise. The reaction mixture was stirred for 2 h at room temperature. Saturated $NaHCO_3$ solution (30 ml) was added and the mixture extracted with diethyl ether (30 ml × 3). The combined organic layers were washed with water, dried over Na_2SO_4, concentrated and chromatographed on silica gel (hexane/ether 3/1, R_f=0.14) to afford 4.53 g (83%) of **3a**. Compounds **3b**, **3c** and **3d** were similarly prepared in 74%, 71% and 66% yield, respectively. **3a**: ^{1}H NMR δ 0.90 (t, 3H, J=7.4 Hz), 1.13 (d, 3H, J=6.2 Hz), 1.40–1.59 (m, 2H), 1.82 (quin, 2H, J=5.6 Hz), 2.64 (br s, OH), 3.33–3.56 (m, 1H), 3.59–3.81 (m, 4H). **3b**: ^{1}H NMR δ 0.91 (t, 3H, J=6.6 Hz), 1.14 (d, 3H, J=6.2 Hz), 1.21–1.56 (m, 4H), 1.82 (quin, 2H, J=5.6 Hz), 2.59 (br s, OH), 3.36–3.45 (m, 1H), 3.81–3.50 (m, 4H). **3c**: ^{1}H NMR δ 0.90 (t, 3H, J=6.6 Hz), 1.14 (d, 3H, J=6.2 Hz), 1.27–1.55 (m, 6H), 1.82 (quin, 2H, J=5.6 Hz), 2.64 (br s, OH), 3.37–3.53 (m, 1H), 3.57–3.80 (m, 4H). **3d**: ^{1}H NMR δ 0.90 (t, 3H, J=6.4 Hz), 1.15 (d, 3H, J=6.2 Hz), 1.22–1.54 (m, 8H), 1.83 (quin, 2H, J=5.6 Hz), 2.38 (br s, OH), 3.31–3.44 (m, 1H), 3.48–3.82 (m, 4H).

2.2.3. Mesylates, 4. To an ether (100 ml) solution of the alcohol **3a** (4.31 g, 32.6 mmol) were added triethylamine (6.62 g, 60.2 mmol) and methanesulphonyl chloride (7.46 g, 65.2 mmol) in ether (15 ml). The mixture was stirred overnight at room temperature. To this solution was added water (100 ml) and the product was extracted with diethyl ether (30 ml × 3). The combined organic layers were dried (Na_2SO_4) and evaporated to give 5.60 g (82%) of mesylate **4a**. The mesylates **4b**, **4c** and **4d** were similarly prepared in 99%, 99%, and 99% yield, respectively. **4a**: ^{1}H NMR δ 0.89 (t, 3H, J=7.4 Hz), 1.11 (d, 3H, J=6.2 Hz), 1.38–1.57 (m, 2H), 1.98 (quin, 2H, J=6.2 Hz), 3.01 (s, 3H), 3.27–3.40 (m, 1H), 3.43–3.61 (m, 2H), 4.34 (t, 2H, J=6.2 Hz). **4b**: ^{1}H NMR δ 0.91 (t, 3H, J=6.6 Hz), 1.13 (d, 3H, J=6.2 Hz), 1.21–1.53 (m, 4H), 1.99 (quin, 2H, J=6.2 Hz), 3.01 (s, 3H), 3.38–3.62 (m, 3H), 4.35 (t, 2H, J=6.2 Hz). **4c**: ^{1}H NMR δ 0.90 (t, 3H, J=6.6 Hz), 1.12 (d, 3H, J=6.2 Hz), 1.17–1.54 (m, 6H), 1.98 (quin, 2H, J=6.2 Hz), 3.01 (s, 3H), 3.36–3.62 (m, 3H), 4.34 (t, 2H, J=6.2 Hz). **4d**: ^{1}H NMR δ 0.90 (t, 3H, J=6.4 Hz), 1.13 (d, 3H, J=6.2 Hz), 1.22–1.54 (m, 8H), 2.02 (quin, 2H, J=6.2 Hz), 3.02 (s, 3H), 3.39–3.62 (m, 3H), 4.36 (t, 2H, J=6.2 Hz).

2.2.4. (*S*)-3-(2-Alkoxy)-1-bromopropanes, 5. A mixture of mesylate **4a** (5.60 g, 26.6 mmol) and LiBr (7.00 g, 78.8 mmol) in acetone (100 ml) was heated at reflux for 12 h. The solvent was removed on a rotary evaporator to give about 25 ml of reaction mixture. To this was added water (50 ml) and the product was extracted with diethyl ether (30 ml × 3). The combined organic layers were washed with water, dried (Na_2SO_4), and concentrated to give 4.30 g (80%) of **5a**. Bromides **5b**, **5c** and **5d** were similarly prepared in 79%, 99% and 99% yield, respectively. **5a**: ^{1}H NMR δ 0.90 (t, 3H, J=7.4 Hz), 1.19 (d, 3H, J=6.2 Hz), 1.42–1.89 (m, 2H), 2.02–2.17 (m, 2H), 3.31–3.63 (m, 5H). **5b**: ^{1}H NMR δ 0.91 (t, 3H, J=6.6 Hz), 1.13 (d, 3H, J=6.2 Hz), 1.21–1.55 (m, 4H), 1.96–2.16 (m, 2H), 3.38–3.69 (m, 5H). **5c**: ^{1}H NMR δ 0.90 (t, 3H, J=6.6 Hz), 1.12 (d, 3H, J=6.6 Hz), 1.17–1.39 (m, 6H), 1.99–2.17 (m, 2H), 3.41–3.65 (m, 5H). **5d**: ^{1}H NMR δ 0.90 (t, 3H, J=6.4 Hz), 1.14 (d, 3H, J=6.2 Hz), 1.19–1.54 (m, 8H), 2.01–2.19 (m, 2H), 3.38–3.67 (m, 5H).

2.2.5. 4-Alkoxyacetanilides, 7. A mixture of 4-acetamidophenol **6** (3.33 g, 22.0 mmol), bromide **5a** (4.30 g, 22.0 mmol) and potassium carbonate (9.13 g, 66.1 mmol) in 65 ml of acetone was heated under reflux overnight. The solvent was removed on a rotary evaporator to give about 30 ml of mixture. To this solution was added water (30 ml) and the product was extracted with diethyl ether (20 ml × 3). The combined organic layers were dried (Na_2SO_4), concentrated, and chromatographed on silica gel (hexane/ether 1/1, R_f=0.48) to give 3.23 g (56%) **7a**. The acetanilides **7b**, **7c** and **7d** were similarly prepared in 72%, 65% and 63% yield, respectively. **7a**: ^{1}H NMR δ 0.89 (t, 3H,

J=7.4 Hz), 1.13 (d, 3H, J=6.2 Hz), 1.18–1.63 (m, 2H), 2.03 (quin, 2H, J=6.2 Hz), 2.17 (s, 3H), 2.65 (br s, NH), 3.29–3.69 (m, 3H), 4.05 (t, 2H, J=6.2 Hz), 6.87 (d, 2H, J=8.8 Hz), 7.39 (d, 2H, J=8.8 Hz). **7b**: ^{1}H NMR δ 0.89 (t, 3H, J=6.6 Hz), 1.12 (d, 3H, J=6.2 Hz), 1.18–1.51 (m, 4H), 2.01 (quin, 2H, J=6.2 Hz), 2.16 (s, 3H), 2.65 (br s, NH), 3.38–3.69 (m, 3H), 4.04 (t, 2H, J=6.2 Hz), 6.86 (d, 2H, J=8.8 Hz), 7.38 (d, 2H, J=8.8 Hz). **7c**: ^{1}H NMR δ 0.87 (t, 3H, J=6.6 Hz), 1.12 (d, 3H, J=6.2 Hz), 1.18–1.43 (m, 6H), 2.01 (quin, 2H, J=6.2 Hz), 2.16 (s, 3H), 2.64 (br s, NH), 3.36–3.62 (m, 3H), 4.04 (t, 2H, J=6.2 Hz), 6.86 (d, 2H, J=8.8 Hz), 7.38 (d, 2H, J=8.8 Hz). **7d**: ^{1}H NMR δ 0.89 (t, 3H, J=6.4 Hz), 1.13 (d, 3H, J=6.2 Hz), 1.19–1.39 (m, 8H), 2.04 (quin, 2H, J=6.2 Hz), 2.17 (s, 3H), 2.65 (br s, NH), 3.37–3.77 (m, 3H), 4.05 (t, 2H, J=6.2 Hz), 6.87 (d, 2H, J=8.8 Hz), 7.39 (d, 2H, J=8.8 Hz).

2.2.6. 4-Alkoxyanilines, 8. An ethanol (75 ml) solution of **7a** (3.20 g, 12.0 mmol) and a catalytic amount of conc. HCl was stirred at 70°C. After 2 days, the solvent was evaporated *in vacuo*; saturated $NaHCO_3$ (30 ml) was added to the residue. The mixture was extracted with diethyl ether (25 ml × 3) and the combined ether extracts were dried (Na_2SO_4), concentrated, and chromatographed on silica gel (hexane/ether 2/1, R_f=0.24) to afford the 4-alkoxyaniline **8a** (1.45 g, 53%). The anilines **8b**, **8c** and **8d** were similarly prepared in 60%, 37% and 40% yield, respectively. **8a**: ^{1}H NMR δ 0.90 (t, 3H, J=7.4 Hz), 1.13 (d, 3H, J=6.2 Hz), 1.36–1.53 (m, 2H), 2.01 (quin, 2H, J=6.2 Hz), 3.31–3.60 (m, 5H, C<u>H$_2$</u>OC<u>H$_2$</u>, N<u>H</u>), 4.01 (t, 2H, J=6.2 Hz), 6.68 (d, 2H, J=8.8 Hz), 6.77 (d, 2H, 8.8 Hz). **8b**: ^{1}H NMR δ 0.90 (t, 3H, J=6.6 Hz), 1.12 (d, 3H, J=6.2 Hz), 1.18–1.55 (m, 4H), 2.00 (quin, 2H, J=6.2 Hz), 3.35 (br s, NH_2), 3.41–3.69 (m, 3H), 4.00 (t, 2H, J=6.2 Hz), 6.66 (d, 2H, J=8.8 Hz), 6.67 (d, 2H, J=8.8 Hz). **8c**: ^{1}H NMR δ 0.89 (t, 3H, J=6.6 Hz), 1.13 (d, 3H, J=6.2 Hz), 1.18–1.57 (m, 6H), 2.00 (quin, 2H, J=6.2 Hz), 3.19 (br s, NH_2), 3.34–3.43 (m, 1H), 3.47–3.72 (m, 2H), 4.00 (t, 2H, J=6.2 Hz), 6.66 (d, 2H, J=8.8 Hz), 6.77 (d, 2H, J=8.8 Hz). **8d**: ^{1}H NMR δ 0.89 (t, 3H, J=6.4 Hz), 1.12 (d, 3H, J=6.2 Hz), 1.18–1.57 (m, 8H), 2.00 (quin, 2H, J=6.4 Hz), 3.19 (br s, NH_2), 3.34–3.47 (m, 1H), 3.50–3.71 (m, 2H), 4.00 (t, 2H, J=6.2 Hz), 6.72 (d, 2H, J=8.8 Hz), 6.78 (d, 2H, J=8.8 Hz).

2.2.7. 1,3-Phenylene bis[4-(4-alkoxyphenyliminomethyl)] benzoates, 10. A solution of **8a** (1.43 g, 6.4 mmol) and bisaldehyde **9** (1.20 g, 3.2 mmol) in chloroform (100 ml) was heated under reflux for 4 h. The reaction mixture was concentrated and recrystallized from chloroform/ethanol to give **10a** (1.78 g, 71%) as yellow crystals. Final compounds **10b**, **10c** and **10d** were similarly prepared in 78%, 72% and 80% yield, respectively. **10a**: ^{1}H NMR δ 0.90 (t, 6H, J=7.4 Hz), 1.14 (d, 6H, J=6.2 Hz), 1.27–1.55 (m, 4H), 2.06 (quin, 4H, J=6.2 Hz), 3.30–3.56 (m, 2H), 3.59–3.90 (m, 4H), 4.12 (t, 4H, J=6.2 Hz), 6.98 (d, 4H, J=8.8 Hz), 7.20–7.33 (m, 7H), 7.52 (t, 1H, J=8.8 Hz), 8.04 (d, 4H, J=8.4 Hz), 8.30 (d, 4H, J=8.4 Hz), 8.60 (s, 2H). ^{13}C NMR δ 9.76, 19.2, 29.2, 30.1, 64.6, 65.3, 76.6, 115.1, 115.7, 119.2, 122.4, 128.5, 129.9, 130.5, 130.9, 141.1, 143.9, 151.4, 156.2, 158.4, 164.3. HRMS: calcd for $C_{48}H_{52}N_2O_8$ 784.3724; found 784.3726. **10b**: ^{1}H NMR δ 0.90 (t, 6H, J=6.6 Hz), 1.14 (d, 6H, J=6.2 Hz), 1.27–1.55 (m, 8H), 2.06 (quin, 4H, J=6.2 Hz), 3.38–3.75 (m, 6H), 4.11 (t, 4H, J=6.2 Hz), 6.97 (d, 4H, J=8.8 Hz), 7.20–7.33 (m, 7H), 7.52 (t, 1H, J=8.8 Hz), 8.04 (d, 4H, J=8.4 Hz), 8.30 (d, 4H, J=8.4 Hz), 8.59 (s, 2H). ^{13}C NMR δ 14.1, 18.7, 19.6, 30.1, 38.9, 64.6, 65.3, 75.4, 115.1, 115.7, 119.2, 122.4, 128.5, 129.9, 130.5, 130.9, 141.1, 143.9, 151.4, 156.2, 158.4, 164.3. HRMS: calcd for $C_{50}H_{56}N_2O_8$ 812.4037; found 812.4030. **10c**: ^{1}H NMR δ 0.88 (t, 6H, J=6.6 Hz), 1.14 (d, 6H, J=6.2 Hz), 1.29–1.53 (m, 12H), 2.06 (quin, 4H, J=6.2 Hz), 3.31–3.48 (m, 2H), 3.49–3.76 (m, 4H), 4.12 (t, 4H, J=6.2 Hz), 6.97 (d, 4H, J=8.8 Hz), 7.21–7.39 (m, 3H), 7.52 (t, 1H, J=8.8 Hz), 8.04 (d, 4H, J=8.4 Hz), 8.30 (d, 4H, J=8.4 Hz), 8.59 (s, 2H). ^{13}C NMR δ 14.0, 19.6, 22.7, 27.7, 30.1, 36.3, 64.6, 65.3, 75.6, 115.1, 115.7, 119.2, 122.4, 128.5, 129.9, 130.5, 130.9, 141.1, 143.9, 151.4, 156.2, 158.4, 164.3. HRMS: calcd for $C_{52}H_{60}N_2O_8$ 840.4350; found 840.4341. **10d**: ^{1}H NMR δ 0.88 (t, 6H, J=6.4 Hz), 1.15 (d, 6H, J=6.2 Hz), 1.22–1.68 (m, 16H), 2.06 (quin, 4H, J=6.2 Hz), 3.36–3.45 (m, 2H), 3.51–3.79 (m, 4H), 4.12 (t, 4H, J=6.2 Hz), 6.98 (d, 4H, J=8.8 Hz), 7.20–7.33 (m, 3H), 7.53 (t, 1H, J=8.8 Hz), 8.05 (d, 4H, J=8.4 Hz), 8.31 (d, 4H, J=8.4 Hz), 8.60 (s, 2H). ^{13}C NMR δ 14.0, 19.7, 22.6, 25.2, 30.1, 31.9, 36.6, 64.9, 65.3, 75.6, 115.1, 115.7, 119.2, 122.4, 128.5, 129.9, 130.5, 130.9, 141.1, 143.9, 151.4, 156.2, 158.4, 164.3. HRMS: calcd for $C_{54}H_{64}N_2O_8$ 868.4663: found 868.4661.

3. Results and discussion

New chiral banana-shaped liquid crystals with chiral 3-(alkoxy)propoxy terminal groups (**10**, P*n*-O-PIMB5*-4O, n=7, 8, 9 and 10) were synthesized and their physical properties investigated by electric and optical measurements. The synthetic route leading to the banana-shaped liquid crystals **10** is shown in scheme 1. The optically pure (*S*)-3-(2-alkoxy)propan-1-ols (**3**) were prepared from the alkylation of (*S*)-2-alkanols **1**, and followed by hydroboration–oxidation. The mesylates produced from the reactions of **3** with

methanesulphonyl chloride in the presence of triethylamine, were converted to the bromides **5** by refluxing in acetone with lithium bromide. Preparation of the final products **10** from the bromides **5** was performed using procedures described in the literature [22].

The mesophase transition temperatures and enthalpies of the new chiral banana-shaped liquid crystals **10** were determined by DSC in conjunction with POM. All the compounds other than **10d** (n=10), enantiotropically show the B2 phase on cooling, and crystallization temperatures decrease as the terminal alkyl chain length increases; **10d** (n=10) appears to have the B7 phase, as will be shown later. Table 1 summarizes the mesomorphic transition temperatures and associated enthalpy changes for the final compounds, where both B2 and B7 are designated as SmCP.

On cooling Pn-O-PIMB5*-4O (n=7, 8 and 9) from the isotropic phase to the B2 phase, only randomly oriented domains of a circular shape are formed. All these compounds always exhibit fringe textures characteristic of $SmC_SP_A^*$ [25] in the absence of an electric field, as shown in figure 1. By applying a rectangular wave electric field, the fringes disappear and domains with an extinction direction parallel to the layer normal emerge. This texture change is similar to the typical B2 phase observed in standard bent-core mesogens [26, 27], and is attributed to electro-optic switching between $SmC_SP_A^*$ and $SmC_AP_F^*$ in the racemic state.

P10-O-PIMB5*-4O exhibited quite different phase behaviour. When the cell was slowly (0.1°C min^{-1}) cooled from the isotropic phase, helical ribbon structures emerged, figure 2 (*a*). The same cooling rate gave circular domains, figure 2 (*b*), if a triangular wave voltage of 50 V_{pp} of 1 Hz was applied during the cooling. By applying an electric field below a threshold field (11.8 V μm^{-1}), the texture scarcely changed and only a slight rotation of extinction brushes was observed. Once the field was higher than the threshold, the birefringence colour changed and a large rotation (about 90°) of the extinction was observed at the field reversal, as shown in figures 2 (*c–e*). This behaviour is quite similar to that observed in MHOBOW by Walba *et al*. [20]. The behaviour is assigned to the B7 phase; i.e. the state shown by figures 2 (*a*) and 2 (*b*) is a polarization-modulated $SmC_SP_F^*$ [28] and that by figures 2 (*c–e*) is a field-induced metastable $SmC_SP_F^*$.

In Pn-O-PIMB5*-4O (n=7–9), the switching current behaviour on applying a triangular wave electric field revealed two switching current peaks in a half cycle, which means that these materials exhibit the antiferroelectric phase. But as shown in figures 3 (*a*) and 3 (*b*), the second peak is very small in P7-PIMB5*-4O (105°C, 100 V_{pp}, 10 Hz) and P8-PIMB5*-4O (90°C, 100 V_{pp}, 10 Hz). At the first switching peak, most of the domains in the cell change from ferroelectric to ferroelectric and the rest of them from ferroelectric to antiferroelectric. At the second switching peak, a small fraction of the antiferroelectric domains switch to ferroelectric. In contrast, P9-PIMB5*-4O (85°C, 100 V_{pp}, 8 Hz) exhibits two sharp switching current peaks in a half cycle on applying a triangular wave electric field, showing a typical antiferroelectric switching current response, figure 3 (*c*). More interestingly, P10-PIMB5*-4O (82°C, 120 V_{pp}, 20 Hz) shows two peaks after fast cooling from the isotropic phase to the B7 phase, but changes to show a single peak, as shown in figure 3 (*d*). The details of this phase will be reported in the near future.

The assignment of the antiferroelectric phase was more clearly made from SHG observations. For P7-PIMB5*-4O, in the absence of a field no SHG was observed, indicating that the ground state is antiferroelectric. On applying a field along the substrate normal, the SHG signal appeared indicating a field-induced antiferroelectric to ferroelectric phase transition. Figure 4 shows the electric field dependence of the SHG intensity in P7-PIMB5*-4O. The field applied was a triangular wave voltage of 10 Hz, the same as that of the switching current measurement of this compound. On decreasing the field from a saturation of about 2 V μm^{-1}, the SHG intensity decreased, but recovered after reversing the field polarity without showing zero

Table 1. Transition temperatures (°C) and enthalpies (ΔH, kJ mol^{-1}) (*in italics*) of new chiral banana-shaped liquid crystals with chiral 3-(alkoxy)propoxy terminal groups (Pn-O-PIMB5*-4O, n=7, 8, 9 and 10, **10a**–**10d**) on cooling.

Compound	I		SmCP		Cr	m.p.
10a (n=7)	•	115.4	•	104.4	•	120.8
		7.61		*10.1*		
10b (n=8)	•	102.6	•	84.1	•	91.9
		6.43		*7.89*		
10c (n=9)	•	100.4	•	79.9	•	91.8
		8.25		*8.23*		
10d (n=10)	•	95.1	•	79.9	•	92.7
		8.53		*12.1*		

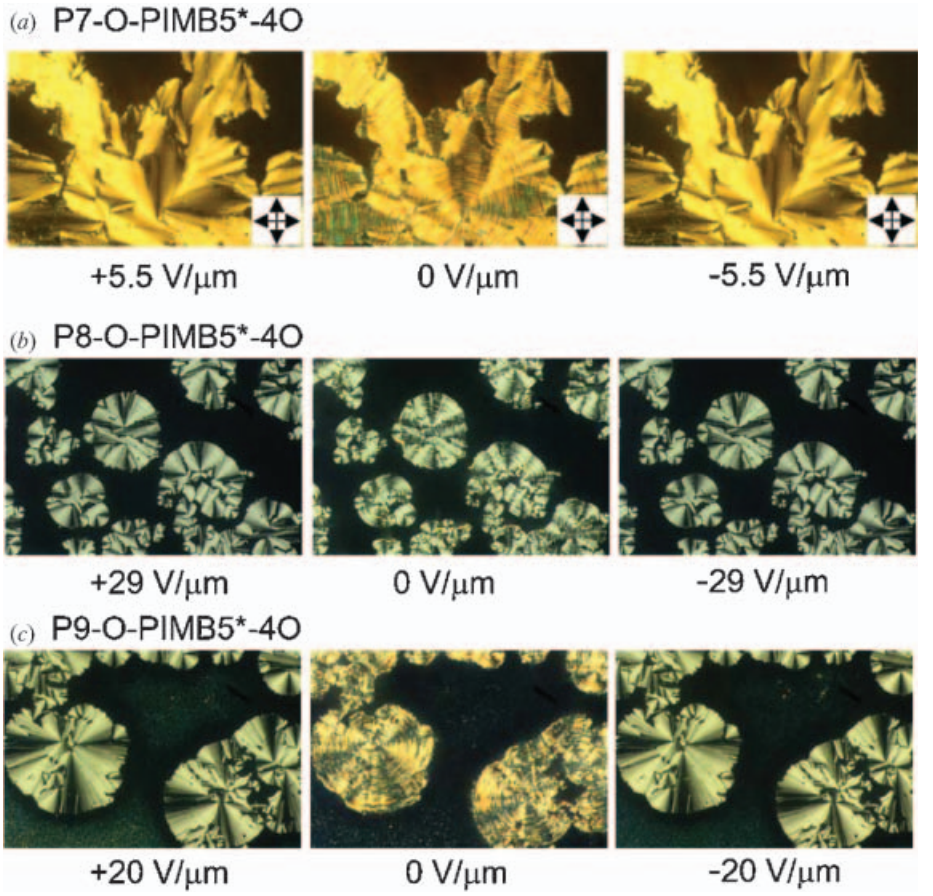

Figure 1. Photomicrographs of the switching behaviour in the B2 phase of P*n*-O-PIMB5*-4O (n=7, 8 and 9): (*a*) 5.5 μm thick P7-O-PIMB5*-4O at 108.9°C, (*b*) 2.1 μm thick P8-O-PIMB5*-4O at 94.0°C, (*c*) 3.0 μm thick P9-O-PIMB5*-4O at 85.0°C. Circular domains of $SmC_SP_A^*$ (E=0 V μm^{-1}) switch to $SmC_AP_F^*$ under the application of an electric field. The polarizer and analyser axes are along the edges of the photos.

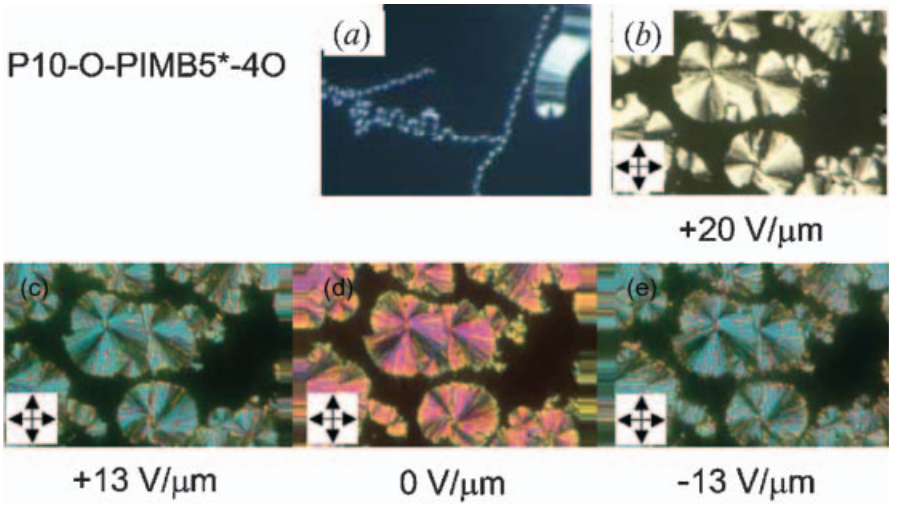

Figure 2. Photomicrographs of the switching behaviour in a 3.8 μm thick P10-O-PIMB5*-4O cell at 85.0°C. (*a*) Texture after slow cooling (0.1°C min^{-1}) from the isotropic phase. (*b*) Texture after slow cooling (0.1°C min^{-1}) from the isotropic phase under the application of a triangular wave voltage (50 V_{pp}) of 1 Hz. The extinction only slightly rotates under a field (6.6 V μm^{-1}) less than a threshold (11.8 V μm^{-1}). (*c*)–(*e*) The texture changes after the application of a high field above the threshold; then the extinction brushes rotationally switch under even a small triangular wave (50 V_{pp}, 1 Hz).

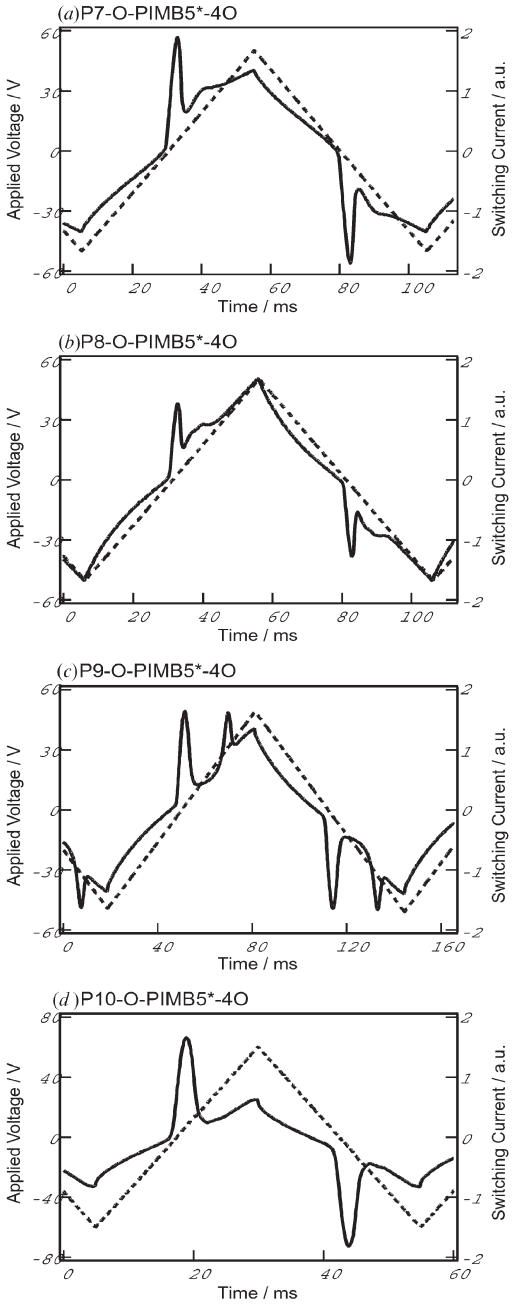

Figure 3. The polarization reversal current in the B2 phase: (*a*) P7-O-PIMB5*-4O at 110.0°C under the application of 100 V_{pp} triangular wave of 10 Hz; (*b*) P8-O-PIMB5*-4O at 90°C under the application of 100 V_{pp} triangular wave of 10 Hz, (*c*) P9-O-PIMB5*-4O at 85.0°C under the application of 100 V_{pp} triangular wave of 8 Hz, (*d*) P10-O-PIMB5*-4O at 82°C under the application of 120 V_{pp} triangular wave of 20 Hz.

SHG intensity. During a.c. field application the signal shows a hysteresis. This result indicates that the stable state of this material is antiferroelectric and a field-induced antiferroelectric to ferroelectric phase transition occurs. Because of the relatively high frequency, however, the direct field-induced transition from the ferroelectric state to the other ferroelectric state occurs dominantly, together with the antiferroelectric to ferroelectric transition. Thus the SHG field dependence is V-shaped with a hysteresis and a finite signal at $\mathbf{E}=0$. This behaviour is consistent with the switching current behaviour shown in figure 3 (*a*); i.e. one dominant current peak and a negligible second peak.

All of the banana-shaped molecules with achiral terminal groups synthesized so far exhibit an antiferroelectric ground state structure. As previously reported [22], SHG studies on the chiral banana-shaped mesogen P7-O-PIMB5* clearly revealed that the stable state is also antiferroelectric and that an electric field-induced antiferroelectric–ferroelectric phase transition occurs with a sharp threshold and a hysteresis. P7-O-PIMB5*-4O and P7-O-PIMB5* have the same terminal chain length and position of the chiral centre. Replacement of one methylene group of the chiral alkyl chain with an oxygen atom does not change the mesomorphic properties, as is expected, because the steric demands of alkyl chains and their oxy-analogues are considered to be nearly the same. The conformational consequence of replacement of a methylene group by an ether oxygen atom has been reviewed: the valency angle and also the preferred conformations and torsional barriers are strikingly preserved [29].

Like P7-O-PIMB5*, P7-O-PIMB5*-4O was, indeed, found to have an antiferroelectic nature by means of electro-optic, polarization reversal current, and SHG measurements. Whereas P8-O-PIMB6* has an inherent ferroelectric property, P8-O-PIMB5*-4O has an

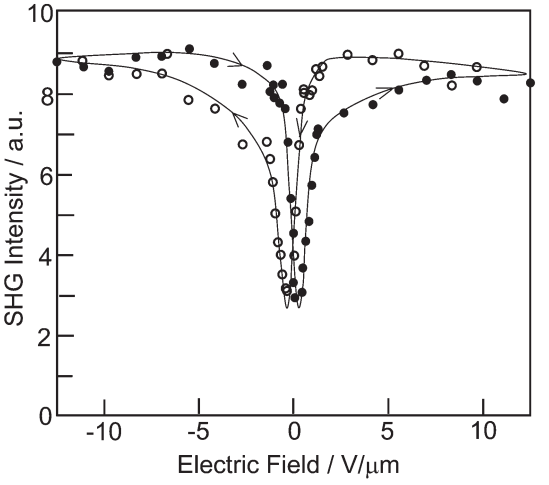

Figure 4. Applied voltage dependence of the SHG intensity in P7-O-PIMB5*-4O. Hysteresis behaviour is seen in the field-induced antiferroelectric–ferroelectric transition.

antiferroelectric phase structure. In these two compounds, every aspect of the structure is the same except for the position of the chiral centre. This leads us to conclude that the structure of terminal chains, especially the position of the chiral centre, plays a key role in the emergence of particular phase structures. The phase structures in the two homologues P*n*-O-PIMB(*n*-2)* and P*n*-O-PIMB(*n*-2)*-(*n*-4)O, which have their chiral centre at the same position in relation to end of the chain, are very similar [24].

4. Conclusion

We have synthesized new chiral banana-shaped liquid crystals with chiral 3-(alkoxy)propoxy terminal groups (P*n*-O-PIMB5*-4O, $n=7$, 8, 9 and 10) and studied their mesomorphic properties and phase structures. Replacement of one methylene group of the chiral alkyl chain with an oxygen atom does not change the mesomorphic properties. This was ascertained by observing that both P7-O-PIMB5*-4O and P7-O-PIMB5* show the same antiferroelectric nature. The position of the chiral centre along the terminal chain plays an important role for the emergence of a particular phase structure. This was ascertained by observing that P8-O-PIMB6* and P8-O-PIMB5*-4O, which are of the same chain length but different chiral centre position, show different phase structures; i.e. ferroelectric and antiferroelectric, respectively.

Acknowledgements

This work is partly supported by Grant-in-Aid for Scientific Research (S) (16105003) from the Ministry of Education, Science, Sports and Culture of Japan. The stay of S. K. L. is supported by JSPS through the TIT-KAIST core university collaboration program. K. T. K. acknowledges PNU for financial support.

References

[1] R.B. Meyer, L. Liebert, L. Strzelecki, P. Keller. *J. Phys. (Fr.) Lett.*, **36**, L69 (1975).
[2] A.D.L. Chandani, E. Gorecka, Y. Ouchi, H. Takezoe, A. Fukuda. *Jpn. J. appl. Phys.*, **28**, L1265 (1989).
[3] T. Niori, T. Sekine, J. Watanabe, T. Furukawa, H. Takezoe. *J. mater. Chem.*, **6**, 1231 (1996).
[4] G. Pelzl, M. Schroeder, U. Dunemann, S. Diele, W. Weissflog, C. Jones, D. Coleman, N. Clark, R. Stannarius, J. Li, B. Das, S. Grande. *J. mater. Chem.*, **14**, 2492 (2004).
[5] M. Nakata, D. Link, J. Thisayukta, Y. Takanishi, K. Ishikawa, J. Watanabe, H. Takezoe. *J. mater. Chem.*, **11**, 2694 (2001).
[6] H. Niwano, M. Nakata, J. Thisayukta, D. Link, H. Takezoe, J. Watanabe. *J. Am. chem. Soc.*, **108**, 14889 (2004).
[7] T. Niori, J. Yamamoto, H. Yokoyama. *Mol. Cryst. liq. Cryst.*, **411**, 1325 (2004).
[8] J. Thisayukta, H. Niwano, H. Takezoe, J. Watanabe. *J. Am. chem. Soc.*, **124**, 3354 (2002).
[9] C.K. Lee, S.S. Kwon, T.S. Kim, E.J. Choi, S.T. Shin, W.C. Zin, D.C. Kim, J.H. Kim, L.C. Chien. *Liq. Cryst.*, **30**, 1401 (2003).
[10] M. Nakata, D.R. Link, F. Araoka, J. Thisayukta, Y. Takanishi, K. Ishikawa, J. Watanabe, H. Takezoe. *Liq. Cryst.*, **28**, 1301 (2001).
[11] J. Thisayukta, H. Niwano, H. Takezoe, J. Watanabe. *J. mater. Chem.*, **11**, 2717 (2001).
[12] M. Nakata, D.R. Link, Y. Takanishi, Y. Takahashi, J. Thisayukta, H. Niwano, D.A. Coleman, J. Watanbe, A. Iida, N.A. Clark, H. Takezoe. *Phys. Rev. E.*, **71**, 011705 (2005).
[13] D.A. Olson, M. Veun, A. Cady, M.V. D'Agostino, P.M. Johnson, H.T. Nguyen, L.C. Chien, C.C. Huang. *Phys Rev. E*, **63**, 041702 (2001).
[14] R. Chistina, R. Amaranatha, H. Harald, L. Heinrich, T. Carsten. *Chem. Commun.* 1898 (2004).
[15] G. Dantgraber, A. Eremin, S. Diele, A. Hauser, H. Kresse, G. Pelzl, C. Tschierske. *Angew. Chem., int. Ed. Engl.*, **41**, 2408 (2002).
[16] H. Nadasi, W. Weissflog, A. Eremin, G. Pelzl, S. Diele, B. Das, S. Grande. *J. mater. Chem.*, **12**, 1316 (2002).
[17] G. Bedel, J.C. Rouillon, J.P. Maroerou, M. Laguerre, H.T. Nguyen, M.F. Achard. *Liq. Cryst.*, **27**, 1411 (2000).
[18] G. Bedel, J.C. Rouillon, J.P. Maroerou, M. Laguerre, H.T. Nguyen, M.F. Achard. *Liq. Cryst.*, **28**, 1285 (2001).
[19] R.A. Reddy, B.K. Sadashiva. *J. mater. Chem.*, **12**, 2627 (2002).
[20] D.M. Walba, E. Korblova, R. Shao, J.E. Maclennan, D.R. Link, M.A. Glaser, N.A. Clark. *Science*, **288**, 2181 (2000).
[21] E. Gorecka, D. Pociecha, F. Araoka, D.R. Link, M. Nakata, J. Thisayukta, Y. Takanishi, K. Ishikawa, J. Watanabe, H. Takezoe. *Phys. Rev. E.*, **62**, 4524 (2000).
[22] K. Kumazawa, M. Nakata, F. Araoka, Y. Takanishi, K. Ishikawa, J. Watanabe, H. Takezoe. *J. mater. Chem.*, **14**, 157 (2004).
[23] F. Araoka, J. Thisayukta, K. Ishikawa, J. Watanabe, H. Takezoe. *Phys. Rev. E.*, **66**, 21705 (2002).
[24] S.K. Lee, S. Heo, J.G. Lee, K.-T. Kang, K. Kumazawa, K. Nishida, Y. Shimbo, Y. Takanishi, J. Watanabe, T. Doi, T. Takahashi, H. Takezoe. *J. Am. Chem. Soc.*, **127**, 11085 (2005).
[25] D.R. Link, G. Natale, R. Shao, J.E. Maclennan, N.A. Clark, E. Korblova, D.M. Walba. *Science*, **278**, 1924 (1997).
[26] M. Zennyoji, Y. Takanishi, K. Ishikawa, J. Thisayukta, J. Watanabe, H. Takezoe. *J. mater. Chem.*, **9**, 2775 (1999).
[27] M. Zennyoji, Y. Takanishi, K. Ishikawa, J. Thisayukta, J. Watanabe, H. Takezoe. *Jpn. J. Appl. Phys.*, **39**, 3536 (2000).
[28] D.A. Coleman, J. Fernsler, N. Chattham, M. Nakata, Y. Takanishi, E. Korblova, D.R. Link, R.-F. Shao, W.G. Jang, J.E. Maclennan, O. Mondainn-Monvaol, C. Boyer, W. Weissflog, G. Pelzl, L.-C. Chien, J. Zasadzinski, J. Watanabe, D.M. Walba, H. Takezoe, N. Clark. *Science*, **301**, 185 (2003).
[29] J. Dale. *Tetrahedron*, **30**, 1683 (1974).